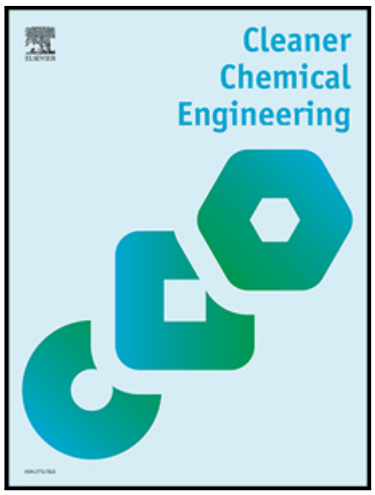

THERMOGRAVIMETRIC ANALYSIS OF CAMEL DUNG, DATE STONE, AND THEIR BLEND FOR PYROLYTIC, KINETIC, AND THERMODYNAMIC STUDIES

Prakash Parthasarathy , Anabel Fernandez , Deepak Kumar Singh , Tareq Al-Ansari , Hamish R. Mackey , Rosa Rodriguez , Germán Mazza , Jeewan Vachan Tirkey , Gordon McKay

PII: S2772-7823(22)00070-5
DOI: https://doi.org/10.1016/j.clce.2022.100072
Reference: CLCE 100072

To appear in: *Cleaner Chemical Engineering*

Received date: 18 August 2022
Revised date: 19 September 2022
Accepted date: 8 October 2022

Please cite this article as: Prakash Parthasarathy , Anabel Fernandez , Deepak Kumar Singh , Tareq Al-Ansari , Hamish R. Mackey , Rosa Rodriguez , Germán Mazza , Jeewan Vachan Tirkey , Gordon McKay , THERMOGRAVIMETRIC ANALYSIS OF CAMEL DUNG, DATE STONE, AND THEIR BLEND FOR PYROLYTIC, KINETIC, AND THERMODYNAMIC STUDIES, *Cleaner Chemical Engineering* (2022), doi: https://doi.org/10.1016/j.clce.2022.100072

THERMOGRAVIMETRIC ANALYSIS OF CAMEL DUNG, DATE STONE, AND THEIR BLEND FOR PYROLYTIC, KINETIC, AND THERMODYNAMIC STUDIES

Prakash Parthasarathy[1*], Anabel Fernandez[2], Deepak Kumar Singh[3], Tareq Al-Ansari[1, 4], Hamish R. Mackey[1], Rosa Rodriguez[2], Germán Mazza[5,6], Jeewan Vachan Tirkey[3], Gordon McKay[1]

[1]*Division of Sustainable Development, College of Science and Engineering, Hamad Bin Khalifa University, Qatar Foundation, Doha, Qatar.*

[2]*Instituto de Ingeniería Química, Facultad de Ingeniería (UNSJ), Grupo Vinculado al PROBIEN (CONICET-UNCo), San Juan, Argentina*

[3]*Department of Mechanical Engineering, Indian Institute of Technology (BHU), Varanasi-221005, India.*

[4]*Division of Engineering Management and Decision Sciences, College of Science and Engineering, Hamad Bin Khalifa University, Qatar Foundation, Doha, Qatar.*

[5]*Instituto de Investigación y Desarrollo en Ingeniería de Procesos, Biotecnología y Energías Alternativas, PROBIEN (CONICET-UNCo), Neuquén, Argentina*

[6]*Centro Científico Tecnológico CONICET - Patagonia Confluencia, Neuquén, Argentina*

[*]*Corresponding author's Email ID: pparthasarathy@hbku.edu.qa*

Highlights

- Pyrolysis behaviour of a novel biomass feedstocks are studied using TGA.
- The pyrolysis kinetics is studied using different models.
- The thermodynamic properties of pyrolysis are determined.

Abstract

Camel dung (CM) and date stone (DS) are biomass resources that are abundant across the Gulf region and have the potential to produce sustainable renewable fuels and specialty products. Copyrolysis of camel dung with DS is an intriguing research approach to boosting both the

production and quality of pyrolysis products, particularly biochar. The current study investigated the bio-energy potential of CM, DS, and CD-DS blend by assessing their physicochemical attributes, pyrolysis characteristics, and kinetic behaviour using thermodynamic analysis. To investigate the pyrolysis behaviour, the materials were thermally decomposed using a thermogravimetric analyser under non-isothermal conditions at different heating rates in a nitrogen environment. The findings of the physicochemical analysis established the bio-energy potential of the feedstocks for long-term energy generation. Thermal degradation profiles of the samples revealed multistage degradation due to the various components in their structure. While a positive synergistic effect between DS and CD was observed in the thermal profile of the blend. The average apparent activation energy of CD from the Friedman method, Flynn-Wall-Ozawa (FWO) model, Kissinger-Akahira-Sunose (KAS) method, and Starink model was 324, 167, 157, and 158 kJ/mol, respectively. Friedman, FWO, KAS, and Starink methods yielded average activation energies of 621, 315, 276, and 279 kJ/mol for DS, respectively. The mean activation energy of the blend estimated using the Friedman, FWO, KAS, and Starink methods was 210, 216, 206, and 207 kJ/mol, respectively. The thermodynamic outcomes reveal that slow pyrolysis of the specified feedstocks is a nonspontaneous process requiring external energy for their degradation. The findings of this study may aid in a better understanding of reaction processes and the expansion of pyrolysis applications of DS, CD, and their mix.

Keywords: Camel dung, Date stone, Pyrolysis, Thermogravimetric analysis, Kinetic analysis, Thermodynamic properties.

1. Introduction

Being a hot and dry nation, Qatar produces large amounts of animal waste rather than plant waste. The amount of excrement produced by dairy, goats, sheep, horses, and camels, in particular, is enormous. Camel dung (CD) is distinctive among manures in that it may be burnt directly to produce heat because of its low moisture and high carbon content. A survey reports that Qatar has over 120,000 camels (PSA, 2018). Given that each adult camel excretes about one tonne of dung per year, the country produces over 120,000 tonnes of CD each year (Parthasarathy et al., 2021).

The *Phoenix dactylifera* often known as 'date palm' is a tropical species native to the Arabian Peninsula with a 7000-year history of cultivation (Chandrasekaran and Bahkali, 2013). Proteins, carbohydrates, mineral salts, vitamins, amino acids, fatty acids, and fibres are abundant in date fruits. Because of their great nutritional content, they are a major part of the Arab community's diet. Dates are used to make a variety of products, including date syrups, date vinegar, date pastes, and date wine. The date fruit has a seed which is also high in carbohydrate, protein, fibre, mineral salts, and vitamin nutrients. Around 8.6 million tonnes of date fruits are harvested worldwide annually (FAO, 2020) while in the state of Qatar, around 30000 tonnes of date fruits are cultivated (PSA, 2018). Assuming that date seed make between 8 and 15% of the weight of the fruit, Qatar's DS supply is projected to be around 3000 tonnes (Demirbas, 2017).

DS and CD are both good sources of energy and chemicals (Hijab et al., 2021). Valorisation processes such as fermentation, anaerobic digestion, pyrolysis, composting, liquefaction, and gasification are commonly used to extract energy/fuels/chemicals from organic waste materials (Alherbawi et al., 2021; Parthasarathy et al., 2017; Singh and Tirkey, 2021). Among these methods, only pyrolysis produces solid, liquid, and gaseous products in

considerable amounts (Gupta et al., 2016). Even though three forms of pyrolysis are available, this research only looks at the slow pyrolysis method of feedstock valorisation.

Copyrolysis is a pyrolysis method that uses at least two carbon-rich materials as a feedstock. Organic materials such as coal, agricultural waste, animal manure, and municipal garbage are often used as feedstocks for copyrolysis. This process has the key benefit of effectively addressing waste disposal issues since it can treat many waste materials at once. Another advantage is that it assures a steady supply of feedstock. DS waste is scarce in Qatar, but CD waste is profuse; consequently, mixing DS and CD waste will assure a long-term accessibility of pyrolysis feedstocks. Another distinguishing aspect of copyrolysis is its combined effect, which typically leads to higher product quality and fewer pollutant releases. By combining DS and CD waste, the water content of the blend will be considerably lowered, reducing the expenditure and drying time. In addition, since camel husbandry and date palm tree cultivation are widespread in Qatar, repurposing CD and DS waste might help to safeguard social sustainability by providing new employment.

Biomass components such as moisture, extractives, hemicellulose, cellulose, lignin, and inorganic minerals are found in both plant biomass and herbivore livestock (animals that eat solely plants) dung (Goenka et al., 2015; Wang et al., 2020). The proportion of these components varies depending on the type of biomass and they have a considerable control on the production and dissemination of pyrolysis products in addition to the basic pyrolysis process influencing factors such as pyrolysis temperature, solid and gas residence time, heating rate, and feedstock size (Prakash and Sheeba, 2016). As a result, knowledge of the thermal behaviour of cellulose, hemicellulose, and lignin is crucial before any pyrolysis investigation (Islam et al., 2016), which is frequently acquired via thermogravimetric analysis (TGA). Thermal analysis data is utilized to

calculate kinetic parameters, which may be applied to predict the dynamic characteristics of pyrolysis degradation (Colpani et al., 2022).

Several investigations on thermal analysis of livestock waste have been conducted, including cattle (Otero et al., 2011), horse (Caro and Dahl, 2021), goat (Junhui Zhang et al., 2019), sheep (Akyürek et al., 2021), swine (Cheng et al., 2019) and chicken (Shim et al., 2022). Nonetheless, there is a scarcity on the thermal analysis of CD (Al-Rumaihi et al., 2021; Parthasarathy et al., 2021). On the other hand, many works of literature have been published that look into the TGA of DS (Bensidhom et al., 2021; El may et al., 2012). There is also a wealth of material on the copyrolysis of animal manure and other waste materials. For example, Ro *et al.* looked into the copyrolysis behaviour of chicken manure and rye grass (Ro et al., 2010), Sánchez *et al.* carried out a copyrolysis analysis of cattle manure and sewage sludge (Sánchez et al., 2007) while Xu *et al.* studied copyrolysis of swine manure and corn straw (Xu et al., 2019). However, the TGA of a copyrolysis of CD and DS is, nevertheless, limited. Consequently, this research looked at the TGA of a CD-DS blend.

The goal of this study is to use TGA to: learn about the slow pyrolysis thermal characteristics of CD sample, DS sample, and a CD-DS blend sample; study the synergistic effect of the CD-DS blend sample; determine the kinetic properties of slow pyrolysis using iso-conversional kinetic models such as Flynn-Wall-Ozawa (FWO), Friedman, Starink, and Kissinger-Akahira-Sunose (KAS); estimate the thermodynamic parameters such as enthalpy change, entropy change and change in Gibb's free energy. The study's findings will aid in understanding the pyrolytic attributes of CD, DS, and their blend. Furthermore, knowing pyrolysis process kinetic parameters is critical for pyrolyser design, pyrolysis modelling, and pyrolysis process parameter optimization (Giwa et al., 2018; Ming et al., 2020).

2. Materials and methods

A local camel farm provided the fresh camel (*Camelus dromedarius*) dung. The moisture content of the excrement was measured and determined to be 37.5%. It was then sun-dried for some days until the water content was less than 15%. The DS, on the contrary, were obtained from a syrup manufacturer and rinsed twice in water to eliminate impurities and dirt. The wet stones were subsequently oven-dried at 50°C for around 24 hours. Both the excrement and the DS were crushed into powder in a blender. Until it was needed again, the powder was kept in air-sealed containers. The CD and DS mix samples were made by combining equal parts CD and DS (1:1 wt.).

2.1.Physico-chemical analyses

For the proximate analysis of feedstocks, an SDT-650 Thermogravimetry analyser was employed, while for the ultimate analysis, a Euro-vector Euro EA 3000 CHN elemental analyser was used. ASTM D7582-12 and ASTM D 3176–8 were used to conduct the proximate and ultimate analyses, respectively. The analyses estimates are based on the mean of three measured results for each sample that were below a 5% margin of error. The biochemical investigation of the chosen samples was carried out as reported in the study of Zhu *et al*. (Zhu et al., 2020). The feedstocks' higher heating value (HHV) was calculated using the relationship established by Channiwala and Parikh (Channiwala and Parikh, 2002) which is provided below.

$$HHV\ (\frac{kJ}{kg}) = 349.1\ Carbon + 100.5\ Sulphur + 1178.3\ Hydrogen - 15.1\ Nitrogen - 103.4\ Oxygen - 21.1\ Ash \quad (1)$$

Where carbon, sulphur, hydrogen, nitrogen, and oxygen are elements in % determined from ultimate analysis.

While the lower heating value (LHV) was estimated using the below equation.

$$LHV\ \left(\frac{kJ}{kg}\right) = HHV - h_{steam}(0.09\ Hydrogen + 0.01\ Moisture) \quad (2)$$

Where h_{steam} denotes enthalpy of steam which is given by 2260 kJ/kg.

2.2.TGA

The feedstock samples were sieved on a Haver and Boecker sieving machine employing a 125-micron sieve before TGA. The analysis was performed with an SDT 650 Thermogravimetry Analyzer. Under 100 ml/min of N_2, the samples were heated at 10, 25, and 50°C/min to degrade from ambient temperatures to 950°C. Only samples that passed through 125-micron sieve were used in the study, and each run used roughly 17.00-23.50 mg of samples. The TGA runs were done in triplicate.

2.2.1. Pyrolytic behaviour of feedstock samples

Investigation of the thermal characteristics of the feedstock samples as well as kinetic analyses were done using the TGA data that was obtained at 10°C/min.

2.2.2. Estimation of synergistic effect

By comparing the weight loss from TGA data (ΔW, wt. %) with the experimental and estimated findings, the synergistic effect of CD and DS was explored using the following equation.

$$\Delta W = W_{Exp} - W_{Est} \quad (3)$$

W_{Exp} denotes the actual weight loss % from TGA runs. W_{Est} was estimated from the total weight losses following TGA data of individual CD and DS samples:

$$W_{Est} = x_{CM}W_{CM} + x_{DS}W_{DS} \quad (4)$$

where x_{CM} and x_{DS} are the weight fraction of CD (0.5) and DS (0.5) in the corresponding blend sample. W_{CM} and W_{DS} are the weight loss % of individual CD and DS samples, respectively.

2.2.3. Kinetic studies employing models

The pyrolysis of feedstock samples is represented by the following reaction:

$$Feedstock\ samples \rightarrow Char + Volatiles$$

The pyrolysis process' kinetic equation is as follows:

$$\frac{d\alpha}{dt} = k(T)f(\alpha) \quad (5)$$

Where α denotes the degree of samples conversion, $f(\alpha)$ represents weight loss change of sample undertaking disintegration, and k signifies the rate constant.

According to the Arrhenius equation, the constant k is expressed as

$$k = Ae^{\frac{-E}{RT}} \quad (6)$$

where A refers to frequency factor (s^{-1}), E denotes activation energy (J/mol), R corresponds to universal gas constant (8.314 J/mol K), and T stands for absolute temperature (K).

$\propto$ can be expressed as

$$\alpha = \frac{W_0 - W_t}{W_0 - W_f} \quad (7)$$

Where W_0 is weight of sample before degradation (kg), W_t is the weight of sample which is undergoing degradation at a time 't' (kg), and W_f is the weight of sample after degradation (kg). For the entire degradation temperature range and varied heating rates, the relationship between $f(\alpha)$, A, and E characterizes the status of the pyrolysis process.

The correlation between $f(\alpha)$, A, and E characterises the status of the pyrolysis process for the entire degradation temperature limit and different heating rates. Different kinetic models such as Friedman, FWO, KAS, and Starink were employed to examine the pyrolysis kinetic behaviour of feedstocks in this work. The derivations of the aforementioned models are well established in the works of Fernandez *et al* (Fernandez et al., 2020, 2018, 2016).

The equations of the chosen models are given below.

Friedman model

$$\ln(\beta \frac{d\alpha}{dT}) = \ln[A\ (1-\alpha)^{-n}\ ] - \frac{E}{RT} \quad (8)$$

FWO model

$$ln\beta = \ln \frac{EA}{Rg(\alpha)} - 5.331 - 1.052\ \frac{E}{RT} \quad (9)$$

where $g(\alpha)$ is given by $g(\alpha) = n^{-1}\ (-1 + (1-\alpha)^{-n}$ for an nth order reaction

KAS model

$$ln\frac{\beta}{T^2} = ln\frac{AR}{Eg(\alpha)} - \frac{E}{RT} \quad (10)$$

Starink model

$$\ln\left(\frac{\beta}{T^{1.8}}\right) = -\frac{AE}{RT} + C_1 \quad (11)$$

where $A = 1.0070 - 1.2 * 10^{-5}E$

2.2.4. Determination of Thermodynamic parameters

The thermodynamic parameters (change in enthalpy (ΔH), change in entropy (ΔS), and Gibbs free energy (ΔG)) were determined using the estimated kinetic parameter values. The A values were estimated using the below Kissinger's equation (Guo et al., 2022).

$$A = \frac{\beta E exp\left(\frac{E}{RT_p}\right)}{RT_p{}^2} \quad (12)$$

where T_p is the temperature corresponding to the peak decomposition of samples (K). Equations (11) and (12) are used to calculate the thermodynamic characteristics.

$$\Delta H = E - RT_p \quad (13)$$

$$\Delta G = E + RT_p \ln(\frac{k_b T_p}{hA}) \quad (14)$$

where k_b signifies the Boltzmann constant which is given by 1.38 x 10^{-23} (J/K) and h denotes the Planck constant which equals 6.63 x 10^{-34} (Js).

Equation (13) is used to calculate entropy:

$$\Delta S = \frac{\Delta H - \Delta G}{T_p} \quad (15)$$

To reduce interaction effects, the T_p value was calculated based on the lowest heating rate (*i.e.* 10°C/min). The reason is that increasing heating rates results in more interaction between sample components. The E values obtained from all of the chosen models were used to calculate the values of ΔH, ΔG, and ΔS.

3. Results & discussion

3.1.Proximate, ultimate, biochemical, and heating value analyses

3.1.1. Proximate analysis

The proximate analysis outcome of all the feedstock samples are presented in **Table 1**. The proximate analysis results indicate that CD has a medium volatile (53%) content and a low fixed carbon (10%) composition. But it has a high ash (28%) concentration. On the other hand, DS possesses a high fixed carbon (20%) and volatile (68%) composition. Furthermore, they have a low ash (4%) content. The mixing of CD with DS, showed a noticeable change in fixed carbon (14%) and volatile (59%) composition, as well as a considerable reduction in ash content (18%). This trend clearly shows that combining CD with DS enhances CD properties.

Table 1. The outcome of the proximate analysis.

Components wt. (%)	Feedstock samples*		
	CD	DS	CD- DS blend
Moisture	9.40	7.74	8.21
Volatiles	53.09	68.10	59.24
Fixed carbon*d	9.88	20.41	14.20

Ash	27.63	3.75	18.35
	100.00	100.00	100.00

*- air-dried basis

*d- calculated by difference

The results of the current work's proximate analysis of CD and DS are compared to those of previous studies (**Figure 1-2**).

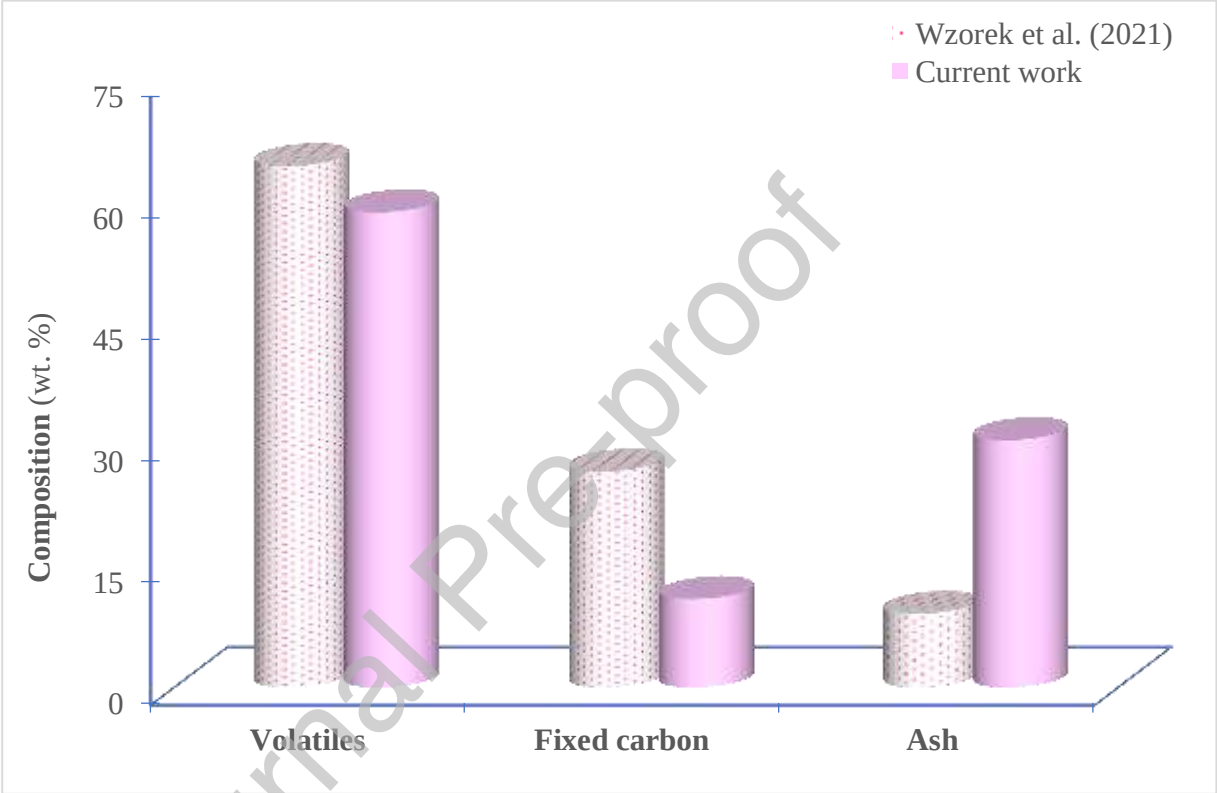

Figure 1. Comparison of proximate analysis results of CD.

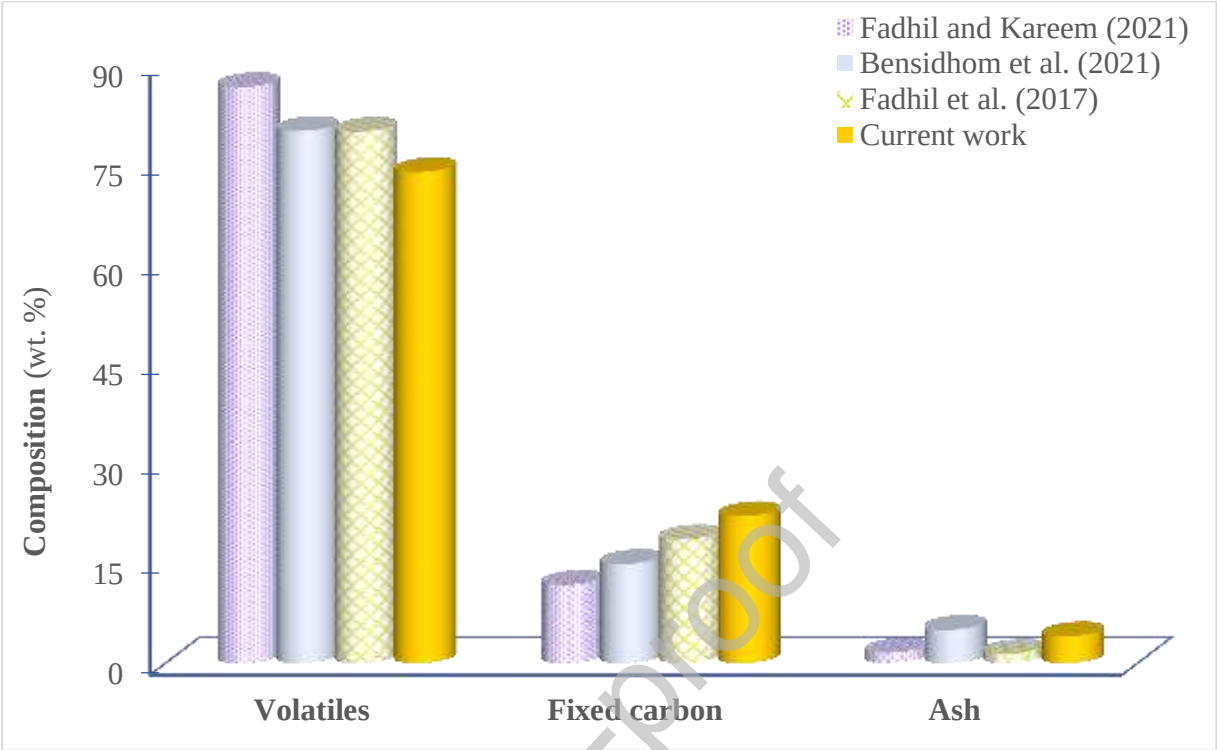

Figure 2. Comparison of proximate analysis results of DS.

Figure 1 shows that the volatile content of the current study is similar to that of Wzorek *et al* (Wzorek et al., 2021). Both works, however, have different fixed carbon and ash contents. **Figure 2** shows that the volatile, fixed carbon, and ash compositions of the current study are consistent with those of previous works (Bensidhom et al., 2021; Fadhil et al., 2017; Fadhil and Kareem, 2021).

3.1.2. Ultimate analysis

Table 2 shows the findings of the ultimate analysis of the feedstock samples. It can be noted that the quality of the CD was improved by the blending, as demonstrated by a raise in carbon composition (from 35 to 41%) and a reduction in volatile composition (from 61 to 53%). It is worth noting that neither CD nor DS contain any sulphur, hence their mixture has no sulphur content.

Table 2. Ultimate analysis outcomes of the feedstock samples.

Components wt. (%)	Feedstock samples*dab		
	CD	DS	CD-DS blend
Carbon	35.33	46.30	40.63
Hydrogen	1.30	6.70	4.55
Nitrogen	2.75	0.83	1.67
Oxygen*d	60.62	46.17	53.15
Sulphur	0.00	0.00	0.00
	100.00	100.00	100.00

*dab- dry and ash-free basis

*d- calculated by difference

The current study's ultimate analysis of CD and DS is compared to prior studies' findings (**Figure 3-4**).

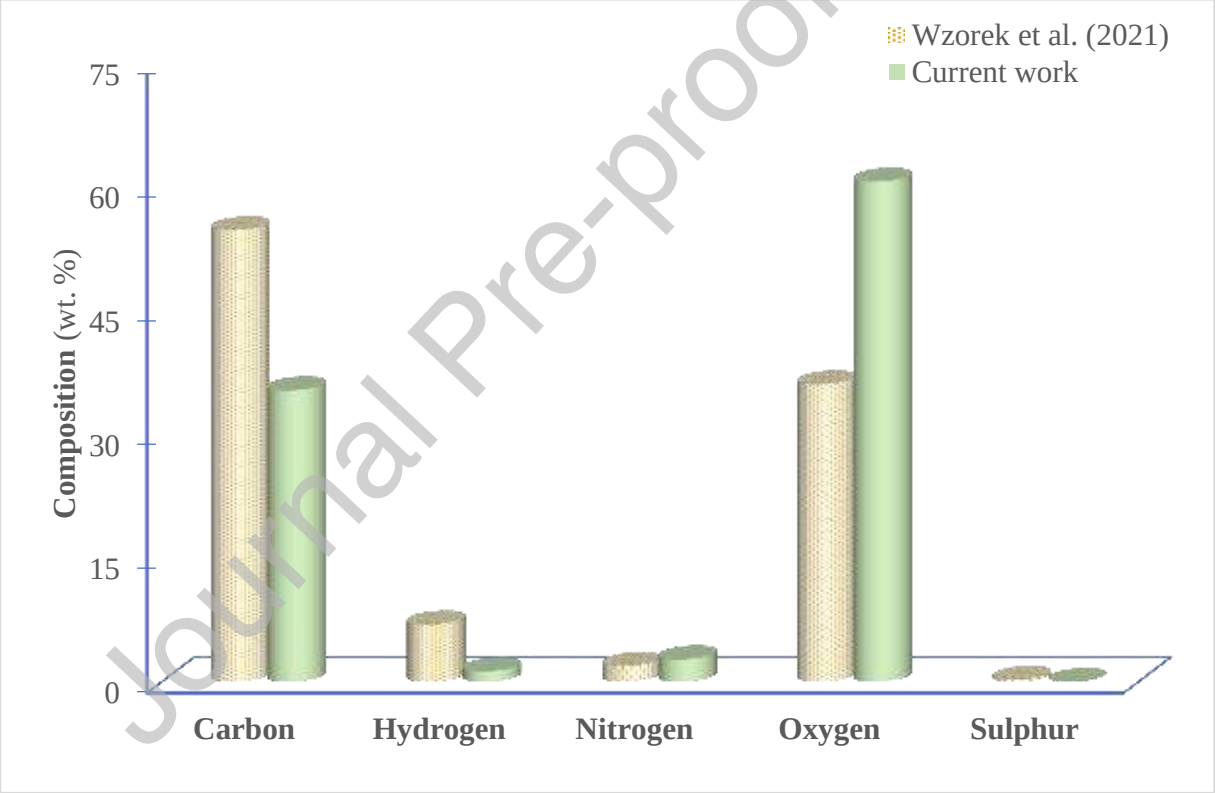

Figure 3. Comparison of ultimate analysis results of CD.

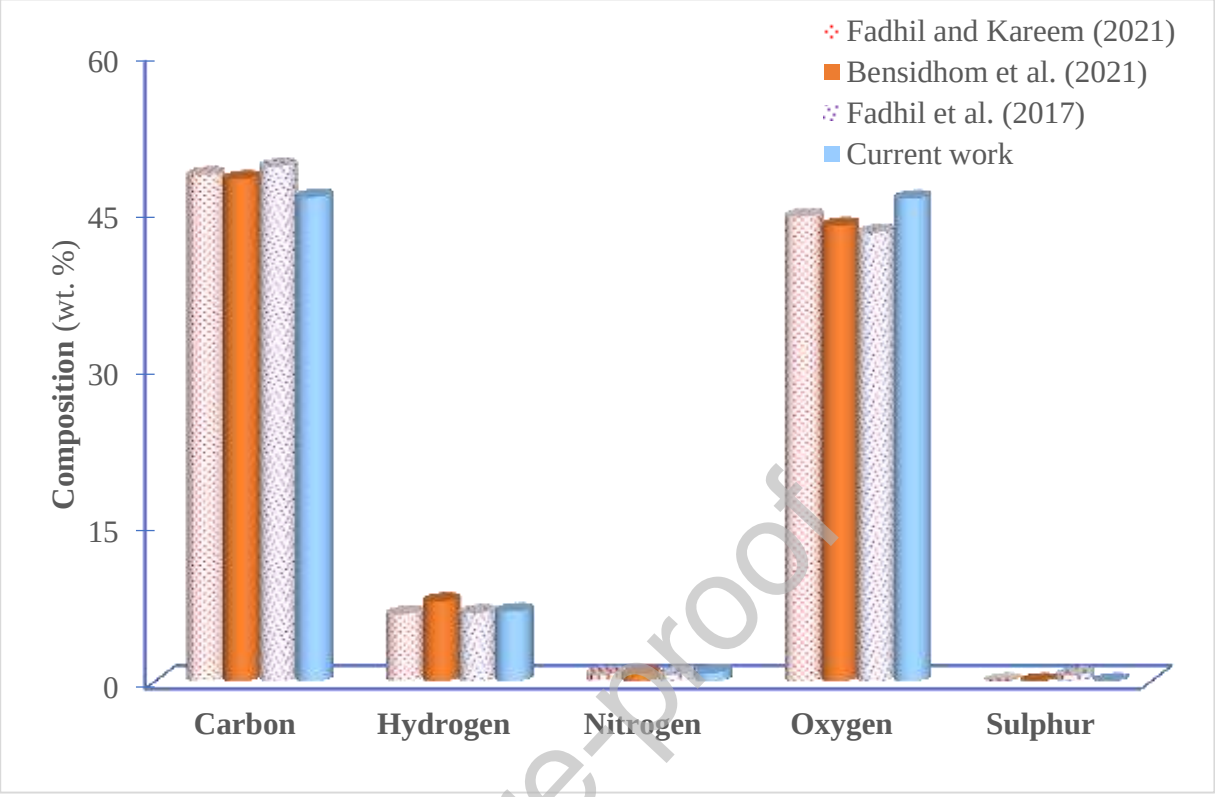

Figure 4. Comparison of ultimate analysis results of DS.

Figure 3 shows a comparison of the current study's CD elemental analysis results with those of Wzorek *et al* (Wzorek et al., 2021). The biochemical compositional results of the CD are comparable to the inference of Wzorek et al., who report that in addition to lignin, cellulose, and hemicellulose, animal manure also contains a significant amount of extractives (such as crude proteins, sugars, fat, *etc*.) as a result of the microbial and chemical activity that occurs in the digestive tract of animals. A considerable change in the elemental composition of carbon, hydrogen, and oxygen may be observed, with the exception of elemental nitrogen and sulphur (Wzorek et al., 2021). **Figure 4** shows, on the other hand, that the current work's ultimate analysis results of DS are compatible with earlier work's findings (Bensidhom et al., 2021; Fadhil et al., 2017; Fadhil and Kareem, 2021). All of the samples' notable cellulose and lignin

contents suggest that they will all produce a appreciable amount of biochar when slowly pyrolyzed.

3.1.3. Biochemical analysis

The outcomes of the biochemical analysis of the feedstock samples are illustrated in **Figure 5**.

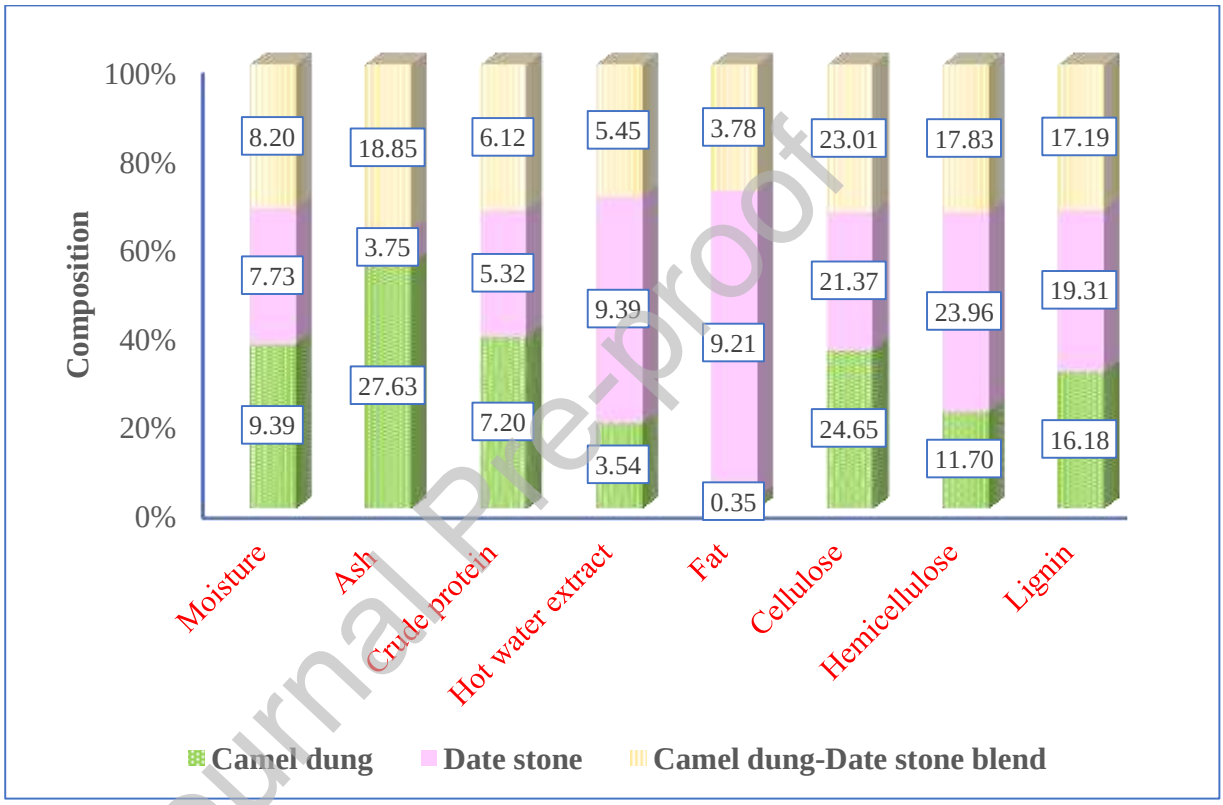

Figure 5. illustrates the results of the biochemical analysis of the samples.

It can be noticed that CD contains slightly more cellulose than DS. DS, instead, contains more lignin and hemicellulose than CD. The blend's cellulose, hemicellulose, and lignin content were comparable to that of CD and DS.

3.1.4. Heating value analysis

Table 3 shows the results of the heating value study of the feedstock samples. The heating value of CD is significantly lower than that of DS, as shown in the table. It is worth mentioning that mixing CD with DS considerably boosted the dung's heating value.

Table 3. The heating value of the feedstock samples.

Heating values (MJ/kg)	Feedstock samples		
	CD	DS	CD-DS blend
HHV	4.18	16.98	9.91
NHV	3.80	15.60	9.05

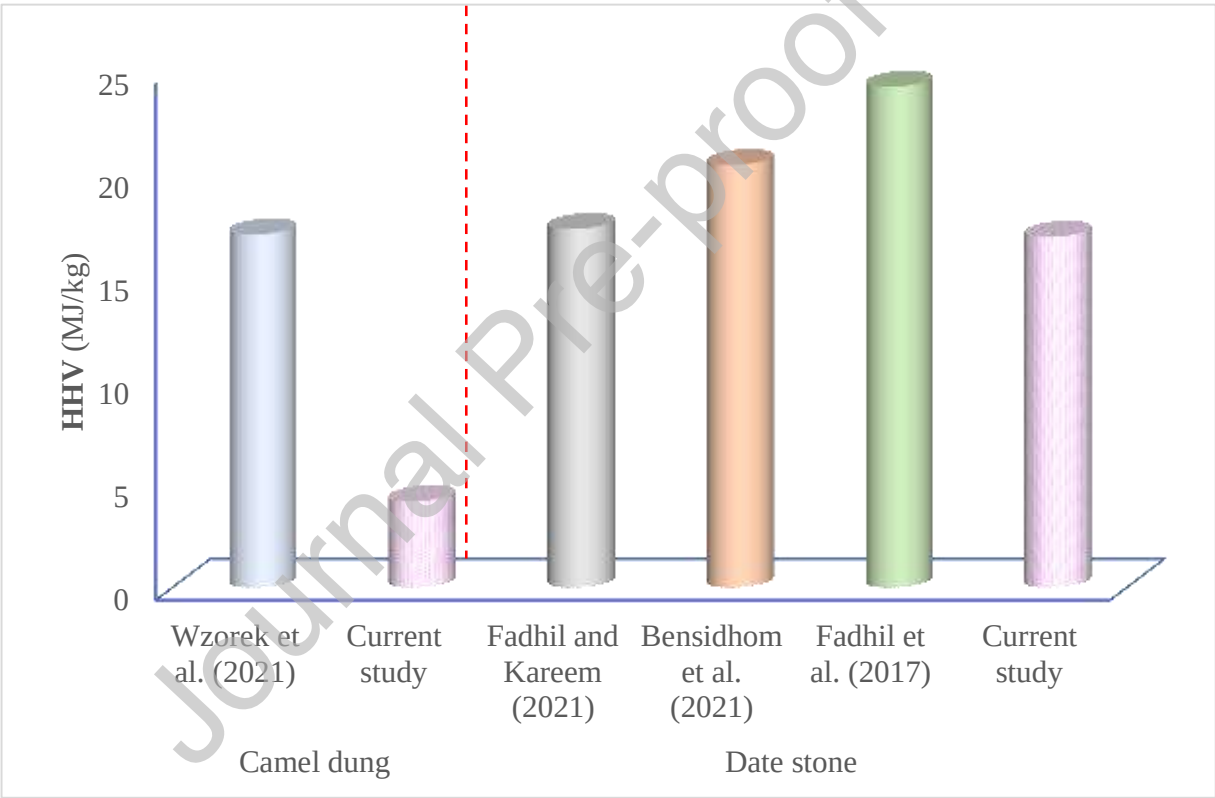

Figure 6. Comparison of ultimate analysis results of DS.

Figure 6. compares the heating value findings of the present work with previous literature investigations. In the case of CD, there is a substantial difference in the heating value based on the current study (Wzorek et al., 2021). Regarding DS, the current findings are consistent with Fadhil and Kareem's research (Fadhil and Kareem, 2021). However, there is a little difference in

the heating value finding between the current study and the studies of Bensidhom *et al*. (Bensidhom et al., 2021) and Fadhil *et al* (Fadhil et al., 2017).

3.2.TGA

3.2.1. Pyrolytic behaviour of feedstock samples

Figures 7 and **8** show the thermogravimetry (TG) and derivative thermogravimetry (DTG) curves of CD, DS, and CD-DS blend produced at 10°C/min.

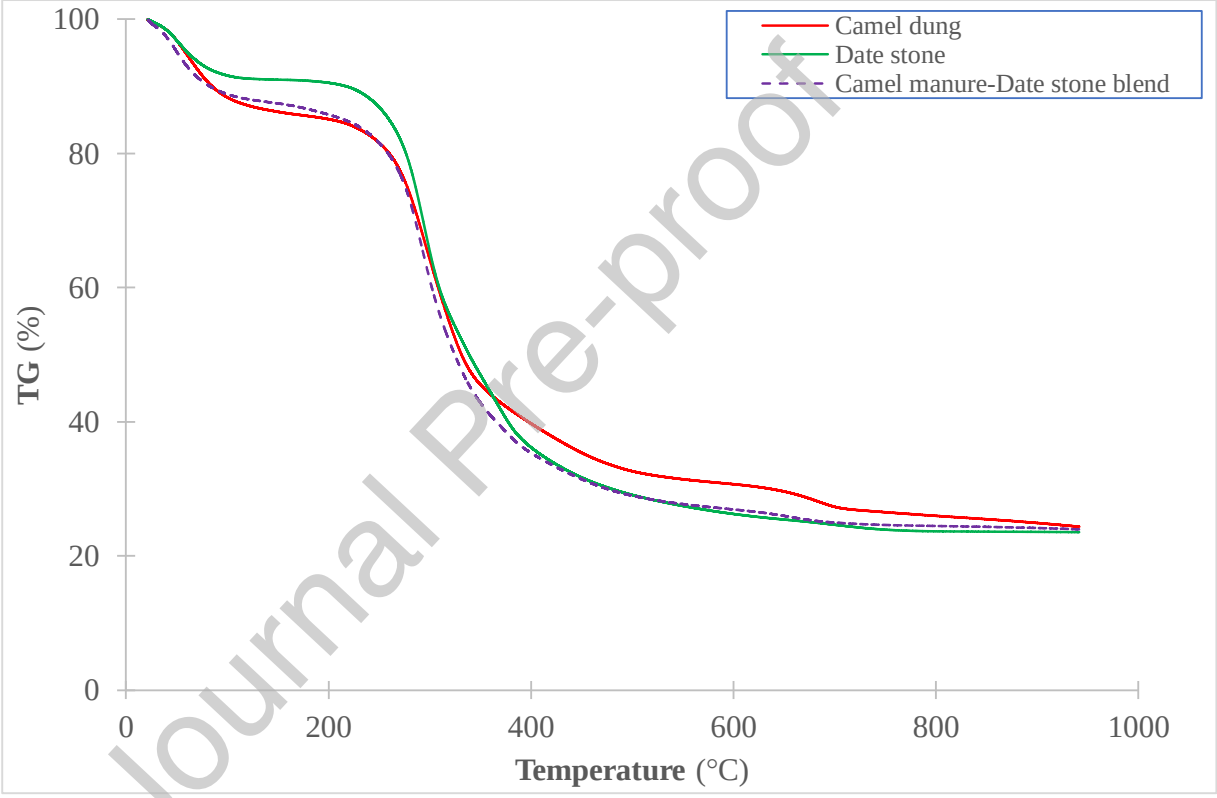

Figure 7. TG curves of the feedstock samples.

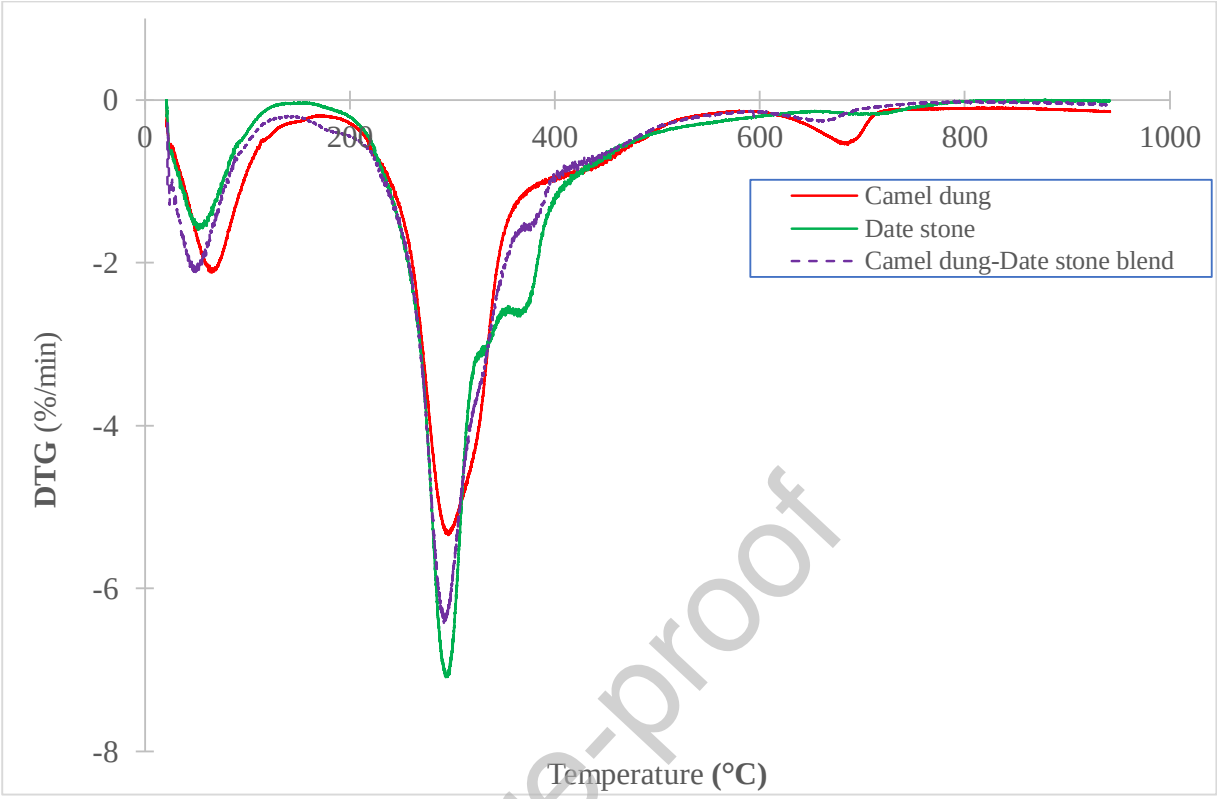

Figure 8. DTG curves of the feedstock samples.

The weight-loss trend of the feedstock samples can be divided into three stages. The first stage is caused by moisture evaporation, as evidenced by the endotherm peak (DTG curves) located between room temperature and 160°C. All of the curves show a steep reduction in weight loss after the first stage. The weight loss in this stage (120-565°C) can be ascribed to the decomposition of cellulose, hemicellulose, lignin, protein, and fat. Even though cellulose, hemicellulose, and lignin disintegrate at this stage, there is only one endotherm visible. This is because the temperature ranges of these biomass components are so close, with cellulose degrading between 250 and 500°C (Parthasarathy et al., 2013), hemicellulose degrading below 350°C (Mishra and Bhaskar, 2014), and lignin degrading between 400°C and 700°C (Sait et al., 2012). The degradation of char formed as a result of the degradation of biomass components can be attributed to the third stage (520-950°C). After the third stage, the leftovers consist of ash and

char residues. **Table 4.** shows the temperature range of the degradation of feedstocks' biomass components.

Table 4.- Pyrolytic degradation behaviour of feedstocks' biomass components.

Feedstock samples	Degradation stages	Biomass components degradation temperature range (°C)	% of weight loss
CD	Stage I- Dehydration	21-117	13.00
	Stage II- Protein, Cellulose, hemicellulose, Lignin	117-565	56.00
	Stage III- Pyrolytic char	565-950	7.00
	Residual	-	24.00
DS	Stage I- Dehydration	Room temperature-160	9.00
	Stage II- Cellulose, hemicellulose, lignin, protein, and fat molecules	160-517	62.00
	Stage III- Pyrolytic char	517-950	5.00
	Residual	-	24.00
CD-DS blend	Stage I- Dehydration	Room temperature-158	13.00
	Stage II- Hemicellulose, cellulose, and lignin components	158-529	59.00
	Stage III- Pyrolytic char	529-950	4.00
	Residual	-	24.00

Using the TG-DTG curves, the feedstock materials' peak degradation temperatures were determined. They are found to be to 300°C, 295°C, and 293°C for CD, DS, and blend respectively. The fact that individual and blend samples had differing peak temperatures demonstrates that blends have a synergistic influence. The change in decomposition % at various phases of degradation (**see Table 4**) validates the presence of the synergistic effect.

The current study's CD degradation characteristics is compared to another study published by Al-Rumaihi *et al* (Al-Rumaihi et al., 2021). I stage: Room temperature-120°C, II stage: 120-567°C, and III stage: 567-950°C were the reported decomposition stages, which are comparable to the current work interpretation. Similarly, when the pyrolytic breakdown behaviour of DS was

analysed, it was found that the decomposition temperature ranges of DS are consistent with the study published by El-May *et al.* (El may et al., 2012), which are I stage: room temperature-170°C, II stage: 170-482°C, and III stage: 482-900°C.

3.2.2. Estimation of synergistic effect

The difference in weight loss (ΔW) can be defined as the synergistic index variable for the copyrolysis of CD and DS to further highlight the synergistic impact between CD biomass and DS. A passive synergistic impact is indicated by ΔW > 0. Meanwhile, ΔW< 0 denotes a faster copyrolysis process and a positive synergistic impact.

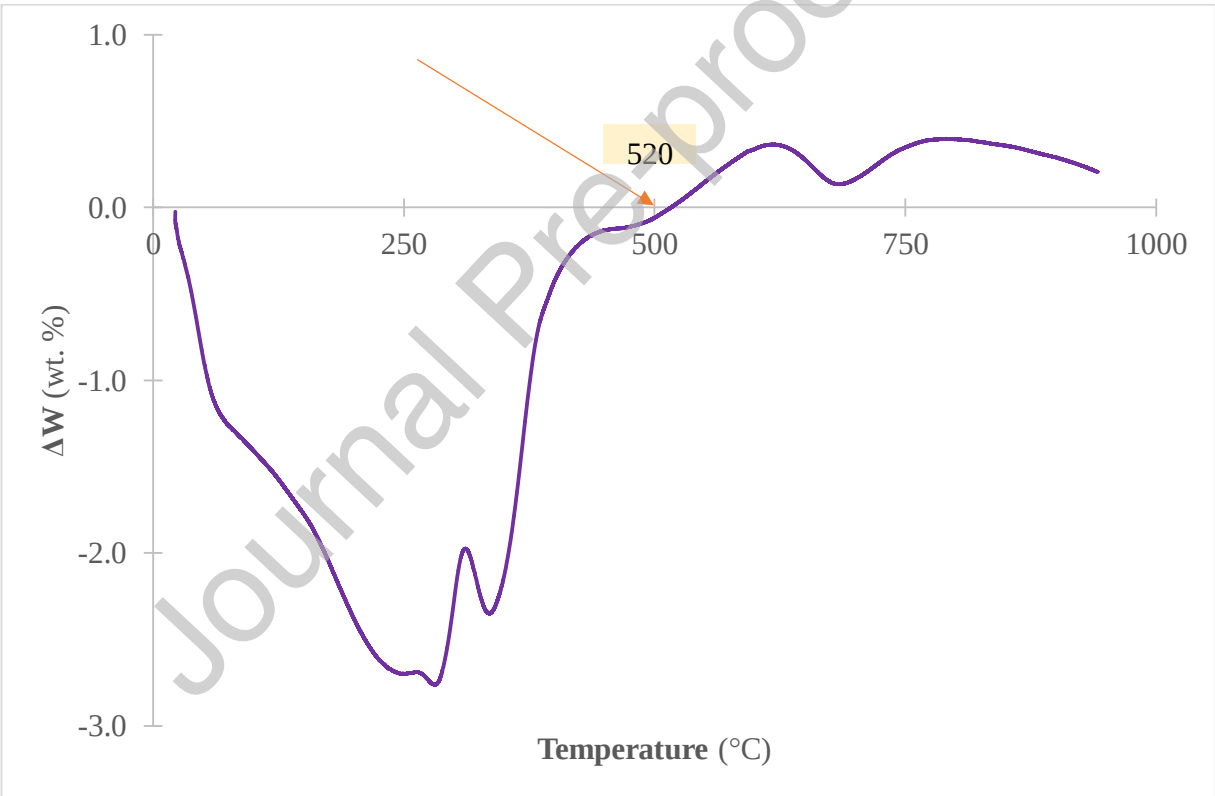

Figure 9. illustrates the change in ΔW with respect to temperature at 10°C/min.

The ΔW is less than -1% until the temperature reaches 50°C. This shows that the estimated and experimental values do not differ significantly in terms of mass loss. This is because pyrolysis does not begin until the temperature reaches 50°C. Up to 520°C, a negative ΔW value

may be found, implying that CD and DS samples have a synergistic relationship and that the pyrolysis process is quick. A positive ΔW value may be seen after 520°C and continues until the completion of the pyrolysis process, demonstrating a passive synergistic effect. It may be deduced that the synergistic influence is greater during the breakdown of hemicellulose, cellulose, and lignin, but the synergistic effect is negligible during the degradation of char.

3.2.3. Kinetic analysis using different models

The pyrolytic kinetics of the CD, DS, and CD-DS blend were determined by using the Friedman, FWO, KAS, and Starink methods at α ranging from 0.1 to 0.8. The iso-conversional lines derived from the four models are presented as supplementary files. The slopes of iso-conversional lines change with the increase of α, and the slopes were utilized to calculate E as shown in **Table 5**.

Table 5. –The E values obtained from the Friedman, FWO, KAS, and Strain models for the pyrolysis of the feedstock samples.

Feedstock	α	Friedman		FWO		KAS		Starink	
		E (kJ/mol)	R^2	E (kJ/mol)	R^2	E (kJ/mol)	R^2	E (kJ/mol)	R^2
CD	0.1	263.63	0.96	126.48	0.90	117.39	0.89	118.22	0.89
	0.2	288.74	0.96	141.62	0.91	132.21	0.90	133.06	0.90
	0.3	304.38	0.96	149.27	0.92	139.67	0.91	140.53	0.91
	0.4	316.35	0.96	155.55	0.91	145.78	0.90	146.65	0.90
	0.5	326.94	0.95	161.53	0.90	151.57	0.89	152.41	0.89
	0.6	340.28	0.95	167.91	0.90	157.75	0.88	158.61	0.88
	0.7	401.36	0.93	184.81	0.88	174.39	0.87	175.23	0.87
	0.8	349.78	0.99	250.66	0.83	239.66	0.81	240.43	0.81
DS	0.1	469.83	0.92	230.11	0.96	196.66	0.98	183.18	0.99
	0.2	473.76	0.98	244.30	0.96	200.68	0.99	203.25	0.99
	0.3	488.51	0.98	271.83	0.94	230.62	0.98	231.57	0.98
	0.4	546.39	0.96	285.38	0.99	245.25	0.97	246.23	0.97
	0.5	699.07	0.89	302.01	0.92	292.18	0.91	293.17	0.91
	0.6	768.59	0.93	379.69	0.83	336.05	0.92	361.29	0.89
	0.7	880.76	0.97	463.21	0.96	376.18	0.99	376.72	0.99
	0.8	642.26	0.99	342.79	0.98	331.86	0.98	333.26	0.98
CD-DS blend	0.1	141.82	0.96	147.02	0.99	138.14	0.99	139.02	0.99
	0.2	181.22	0.99	178.77	0.99	169.48	0.99	170.41	0.99
	0.3	190.88	0.99	193.93	0.99	184.45	0.99	185.39	0.99
	0.4	209.75	0.99	205.95	0.99	196.31	0.99	197.27	0.99
	0.5	235.14	0.99	226.22	0.99	216.42	0.99	217.40	0.99
	0.6	240.44	0.98	251.52	0.99	241.51	0.99	242.50	0.99
	0.7	244.51	0.98	264.14	0.99	253.83	0.99	254.86	0.99
	0.8	237.76	0.99	257.34	0.99	246.51	0.99	247.59	0.99

It should be noted that the E values derived using the FWO, KAS, and Starink models are similar, making these findings comparable. The E values obtained from the Friedman method are greater than the E values produced using the FWO, KAS, and Starink models. A similar behaviour was also observed by Yuan *et al.* (Yuan et al., 2017). Analysing the calculating principles of the four models makes it simple to understand why the differences exist. Some assumptions and approximations are included in the FWO, KAS, and Starink models, but not in the Friedman method (Fernandez et al., 2020). As a result, the values estimated using the Friedman approach are more precise and closer to the real activation energies (Heydari et al., 2015).

With the increase of the α from 0.1 to 0.7, all of the models and feedstock samples displayed a similar shift, with an increasing trend. However, when the α was further increased from 0.7 to 0.8, the E values showed a rising trend in some cases and a declining trend in others. Kumar *et al*. observed an increase in the E value when the α was increased from 0.7 to 0.8 (Kumar et al., 2022) while Al-Rumaihi *et al.* noted a decrease when the α was raised from 0.7 to 0.8 (Al-Rumaihi et al., 2021). The diverse compositions of the samples, which include a very complex matrix of hemicellulose, cellulose, lignin, extractive, and other inorganic compounds, are imputed to the increasing trend of the E values (Mishra and Mohanty, 2020; Özsin and Pütün, 2019). The kinetic data revealed that when the α increased, the E values increased through multiple steps rather than single steps due to the breakdown of organic matter. The activation energy is a barrier that must be overcome before a chemical reaction can begin, and a greater value of E indicates that a reaction will be more difficult to occur. It determines a reaction rate's responsiveness and sensitivity. Hence, it can be inferred that due to high mineral concentrations in all the feedstock samples, the E values in the charring stage (α: 0.7-0.8) are found to be higher.

Friedman, FWO, KAS, and Starink models yielded the E values of 263–401, 126–251, 117–240, and 118–240 kJ mol^{-1}, respectively, for CD. The E values obtained from the Friedman, FWO, KAS, and Starink models in the instance of DS ranged from 470-881, 230–463, 197-376, and 183-376 kJ mol^{-1}, respectively. The activation energy gained from the Friedman, FWO, KAS, and Starink models varied from 142–245, 147–264, 138-254, and 139–255 kJ mol^{-1}, respectively, in the case of the blend.

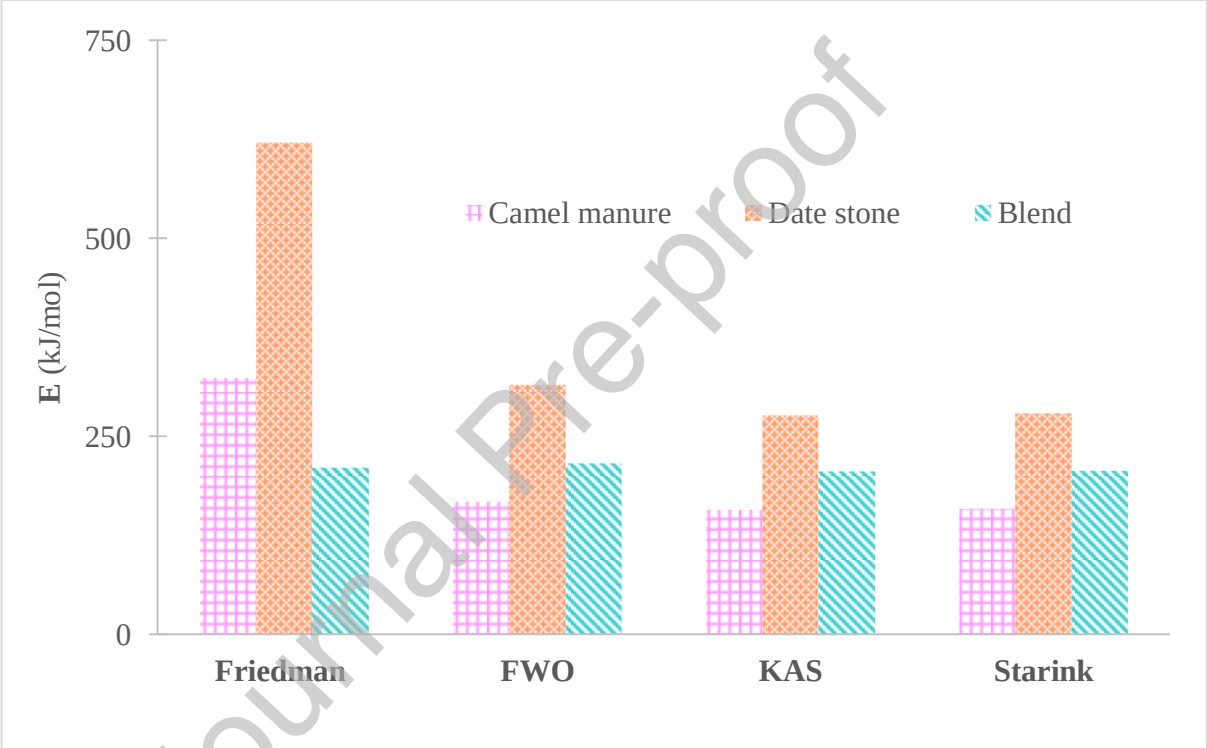

Figure 10. The average E value of feedstock samples.

Figure 10. depicts the average E value of feedstock samples derived using the specified models. The average E value of CD from the Friedman, FWO, KAS, and Starink models is 324, 167, 157, and 158 kJ/mol, respectively. Friedman, FWO, KAS, and Starink models yielded average E values of 621, 315, 276, and 279 kJ/mol for DS, respectively. The average E values of a CD-DS blend calculated using the Friedman, FWO, KAS, and Starink models are 210, 216, 206, and 207 kJ/mol, respectively.

The degradation of the components in biomass is not independent and does not occur in series, as documented in the literature works of Caballero *et al*. (Caballero et al., 1997) and Carrier *et al.* (Marion Carrier et al., 2011). Each component undergoes degradation to variable degrees at different stages, although they all have distinct dominant ranges. As a result, the E values derived in this study should reflect apparent E, a rough estimate, for each component in its dominant ranges. In future studies, it will be fascinating and vital to address the more correct E for each component while considering the coupling relationship between them.

3.2.4. Thermodynamic properties

The outputs of all of the models were consistent with the experimental findings. The thermodynamic parameter values ΔG, ΔH, and ΔS were determined using the E values that were obtained using the specified models. Using the TG-DTG curves (10°C/min), the peak decomposition temperatures for the CD, DS, and blend were noted and they were found to be 296°C, 294°C, and 292°C respectively. **Table 6.** displays the thermodynamic parameter values computed using the Kissinger equation for each of the models listed above.

Table 6. – Thermodynamic parameter values of different models.

Feedstock	Model	α	ΔH (kJ/mol)	A (1/s)	ΔG (kJ/mol)	ΔS (kJ/mol)
CD	Friedman	0.1	258.90	2.55×10^{22}	161.93	0.1704
		0.2	284.00	5.63×10^{24}	161.50	0.2152
		0.3	299.64	1.62×10^{26}	161.25	0.2431
		0.4	311.62	2.11×10^{27}	161.07	0.2645
		0.5	322.21	2.05×10^{28}	160.91	0.2834
		0.6	335.54	3.57×10^{29}	160.72	0.3071
		0.7	396.63	1.70×10^{35}	159.94	0.4158
		0.8	345.05	2.73×10^{30}	160.59	0.3241
	FWO	0.1	121.75	3.17×10^{09}	165.40	-0.0767
		0.2	136.89	8.71×10^{10}	164.87	-0.0492
		0.3	144.54	4.62×10^{11}	164.62	-0.0353
		0.4	150.82	1.82×10^{12}	164.43	-0.0239
		0.5	156.80	6.68×10^{12}	164.25	-0.0131
		0.6	163.18	2.67×10^{13}	164.06	-0.0016

		0.7	180.08	1.05×10^{15}	163.61	0.0289
		0.8	245.93	1.57×10^{21}	162.17	0.1472
		0.1	112.65	4.31×10^{08}	165.76	-0.0933
		0.2	127.48	1.11×10^{10}	165.20	-0.0663
		0.3	134.93	5.68×10^{10}	164.94	-0.0527
		0.4	141.05	2.16×10^{11}	164.73	-0.0416
		0.5	146.84	7.63×10^{11}	164.55	-0.0311
		0.6	153.02	2.93×10^{12}	164.36	-0.0199
		0.7	169.66	1.09×10^{14}	163.88	0.0102
	KAS	0.8	234.93	1.47×10^{20}	162.38	0.1275
		0.1	113.48	5.17×10^{08}	165.72	-0.0918
		0.2	128.33	1.34×10^{10}	165.17	-0.0647
		0.3	135.80	6.86×10^{10}	164.91	-0.0511
		0.4	141.92	2.61×10^{11}	164.70	-0.0400
		0.5	147.68	9.17×10^{11}	164.52	-0.0296
		0.6	153.87	3.53×10^{12}	164.33	-0.0184
		0.7	170.49	1.31×10^{14}	163.86	0.0117
	Starnik	0.8	235.70	1.73×10^{20}	162.37	0.1288
DS		0.1	465.10	3.82×10^{41}	159.20	0.5374
		0.2	469.03	8.85×10^{41}	159.16	0.5444
		0.3	483.77	2.06×10^{43}	159.01	0.5706
		0.4	541.66	4.72×10^{48}	158.48	0.6732
		0.5	694.33	6.21×10^{62}	157.31	0.9435
		0.6	763.86	1.64×10^{69}	156.87	1.0664
		0.7	876.03	3.70×10^{79}	156.22	1.2646
	Friedman	0.8	637.53	3.49×10^{57}	157.72	0.8430
		0.1	225.38	1.87×10^{19}	162.57	0.1104
		0.2	239.57	3.98×10^{20}	162.29	0.1358
		0.3	267.10	1.49×10^{23}	161.78	0.1850
		0.4	280.65	2.74×10^{24}	161.55	0.2092
		0.5	297.28	9.75×10^{25}	161.29	0.2389
		0.6	374.96	1.65×10^{33}	160.20	0.3773
		0.7	458.48	9.31×10^{40}	159.26	0.5257
	FWO	0.8	338.06	6.12×10^{29}	160.69	0.3116
		0.1	191.93	1.36×10^{16}	163.32	0.0503
		0.2	195.94	3.24×10^{16}	163.22	0.0575
		0.3	225.89	2.09×10^{19}	162.56	0.1113
		0.4	240.52	4.89×10^{20}	162.27	0.1375
		0.5	287.45	1.18×10^{25}	161.44	0.2214
		0.6	331.32	1.44×10^{29}	160.78	0.2996
	KAS	0.7	371.45	7.78×10^{32}	160.25	0.3711

		0.8	327.13	5.88×10^{28}	160.84	0.2922
		0.1	178.45	7.35×10^{14}	163.65	0.0260
		0.2	198.52	5.66×10^{16}	163.16	0.0621
		0.3	226.84	2.56×10^{19}	162.54	0.1130
		0.4	241.50	6.03×10^{20}	162.25	0.1392
		0.5	288.44	1.46×10^{25}	161.43	0.2231
		0.6	356.56	3.21×10^{31}	160.44	0.3446
		0.7	371.98	8.72×10^{32}	160.24	0.3720
	Starnik	0.8	328.53	7.93×10^{28}	160.82	0.2946
Blend		0.1	137.09	9.10×10^{10}	164.86	-0.0488
		0.2	176.49	4.80×10^{14}	163.70	0.0225
		0.3	186.15	3.89×10^{15}	163.46	0.0399
		0.4	205.02	2.31×10^{17}	163.01	0.0738
		0.5	230.40	5.53×10^{19}	162.47	0.1194
		0.6	235.71	1.73×10^{20}	162.37	0.1289
		0.7	239.77	4.16×10^{20}	162.29	0.1361
	Friedman	0.8	233.02	9.72×10^{19}	162.42	0.1240
		0.1	142.28	2.83×10^{11}	164.69	-0.0394
		0.2	174.04	2.82×10^{14}	163.77	0.0180
		0.3	189.20	7.54×10^{15}	163.38	0.0454
		0.4	201.21	1.01×10^{17}	163.10	0.0670
		0.5	221.49	8.09×10^{18}	162.65	0.1034
		0.6	246.79	1.89×10^{21}	162.15	0.1487
		0.7	259.41	2.85×10^{22}	161.92	0.1713
	FWO	0.8	252.61	6.60×10^{21}	162.04	0.1591
		0.1	133.40	4.07×10^{10}	164.99	-0.0555
		0.2	164.75	3.76×10^{13}	164.02	0.0013
		0.3	179.71	9.66×10^{14}	163.62	0.0283
		0.4	191.58	1.26×10^{16}	163.32	0.0496
		0.5	211.69	9.75×10^{17}	162.86	0.0858
		0.6	236.77	2.18×10^{20}	162.34	0.1308
		0.7	249.09	3.10×10^{21}	162.11	0.1528
	KAS	0.8	241.78	6.41×10^{20}	162.25	0.1397
		0.1	134.29	4.93×10^{10}	164.96	-0.0539
		0.2	165.68	4.60×10^{13}	163.99	0.0030
		0.3	180.66	1.19×10^{15}	163.60	0.0300
		0.4	192.54	1.55×10^{16}	163.30	0.0514
		0.5	212.67	1.20×10^{18}	162.84	0.0875
		0.6	237.77	2.70×10^{20}	162.32	0.1326
		0.7	250.13	3.87×10^{21}	162.09	0.1547
	Starnik	0.8	242.86	8.09×10^{20}	162.23	0.1417

The A values for all of the models were between 10^8 and 10^{79} s^{-1}, as shown in the table. The values of this range signify that the pyrolysis of the feedstock samples is a complicated process. Surface reactions are typically those with A values $\leq 10^9$ s^{-1} (Di Blasi, 2008). The small A values can be due to a closed junction complex if the reactions are non-surface (independent). Reactions with A values $\geq 10^9$ s^{-1}, on the other hand, imply a more liberal junctional complex (Fernandez et al., 2018). The obtained A values indicate that the materials' pyrolysis of the feedstock materials is a complicated process.

The fact that all α values have positive enthalpy values supports the idea that pyrolysis of the feedstock samples is an endothermic process that requires heat energy to proceed (Fernandez et al., 2020). The ΔH values ranged 113-396, 178-876, and 133-259 kJ/mol for CD, DS, and blend as shown in the table. This indicates that that external energy was spent throughout the pyrolysis process. Furthermore, at the 0.7 and 0.8 values of α, a considerable rise in ΔH values was observed, indicating that a significant quantity of heat energy is spent.

The ΔG values for all conversion fractions in the table are positive. As indicated by the positive ΔG values, the pyrolysis process is an endergonic reaction, requiring a driving force to complete (Guan et al., 2019). The ΔG values were in the range of 159-166, 156-163, and 162-165 kJ/mol for CD, DS, and blend respectively, showing a steady energy output all through the pyrolysis degradation.

Negative ΔS values were found in a few conversion fractions, indicating the creation of active complexes. It is worth noting that only low entropy values were obtained at all conversion fractions, indicating that the pyrolysis process is approaching thermodynamic equilibrium (Müsellim et al., 2018). Furthermore, the ΔS values exhibited a raising trend until the α value is

0.7. Following that, in some circumstances, a decreasing trend may be observed, while in others, an increasing trend may be noted.

The increasing tendency indicates that the feedstock samples are being transformed to biochar, whilst the falling trend indicates that the quantity of unreacted samples is decreasing during the pyrolysis process. The small ΔS values all over the process suggest that the feedstock samples have a low reactivity (Dhyani and Bhaskar, 2018). At 0.7 α, in most cases, maximum ΔS values can be found for all the models and feedstock samples. This indicates a high level of reactivity at this conversion degree. The lowest ΔS value, on the other hand, was achieved at 0.1 conversion fraction, indicating that reactivity is low at this conversion degree.

4. Conclusion

The current study addressed the physicochemical attributes, pyrolytic behaviour, kinetics and thermodynamic analysis of camel dung (CD), date stone (DS), and CD-DS blend using thermogravimetric analysis. The feedstocks' physicochemical study results indicated a huge bioenergy potential for sustainable energy generation. Thermal degradation profiles of the samples revealed degradation of biomass components such as moisture, cellulose, hemicellulose, and lignin, as well as biochar breakdown. Iso-conversional models such as Friedman, Flynn-Wall-Ozawa (FWO), Kissinger-Akahira-Sunose (KAS), and Starink were used to predict the pyrolytic kinetics of the pyrolysis process. The study revealed that the average apparent activation energy changed as the conversion progressed. According to the Friedman, FWO, KAS, and Starink models, the average apparent activation energy of CD was 324, 167, 157, and 158 kJ/mol, respectively. For DS, the Friedman, FWO, KAS, and Starink models produced average activation energies of 621, 315, 276, and 279 kJ/mol, respectively. Using the Friedman, FWO, KAS, and Starink models, the average activation energy of the blend was 210, 216, 206,

and 207 kJ/mol, respectively. The observed frequency factors suggest that pyrolysis of the materials is a complex process. The positive enthalpy values indicate that the pyrolysis of the feedstocks is an endothermic process. The small changes in entropy values indicate that the feedstock samples are reactive. The thermodynamic analysis implies that pyrolysis of CD, DS, and CD-DS blend is extremely feasible.

As demonstrated by the current study, all of the selected feedstock samples are capable of being used in pyrolysis to produce biochar. With the use of CD-DS blend for pyrolysis, CD and DS wastes can be properly disposed of, and biochar will be generated for natural fertiliser production. The current work's outcome presents a new scope for using camel manure as a long-term source for green fuels, and this possibility gives an alternate pathway for CD handling and valorisation. Copyrolysis has the potential to be an alternate waste management approach with substantial implications for waste usage and energy production.

This copyrolysis study may be scaled up to the lab level and subsequently to the industrial level, allowing for the employment of the approach in commercial settings.

Credit authorship contribution statement

Prakash Parthasarathy: Conceptualization, Methodology, Formal analysis, Investigation, Writing – original draft.

Anabel Fernandez: Formal analysis, Investigation, Writing – original draft.

Deepak Kumar Singh: Investigation, Writing – original draft.

Tareq Al-Ansari: Writing - review & editing, Resources.

Hamish R. Mackey: Writing - review & editing, Resources.

Rosa Rodriguez: Writing - review & editing.

Germán Mazza: Writing - review & editing.

Jeewan Vachan Tirkey: Writing - review & editing.

Gordon McKay: Conceptualization, Methodology, Writing – review & editing, Resources, Supervision.

Declaration of Competing Interest

The authors declare that they have no known competing financial interests or personal relationships that could have appeared to influence the work reported in this paper.

Acknowledgement

The authors would like to thank Qatar National Research Fund (QNRF) for their support of this research through NPRP-11S-0117-180328, the Supreme Committee for Delivery and Legacy (SCDL) and Hamad Bin Khalifa University (HBKU) and Qatar Foundation (QF).

Declaration of interests

The authors declare that they have no known competing financial interests or personal relationships that could have appeared to influence the work reported in this paper.

References

1. Akyürek, Z., Singh, R., Strezov, V., 2021. Synergetic Effects during Co-Pyrolysis of Sheep Manure and Recycled Polyethylene Terephthalate. Polymers (Basel). 13, 2363. https://doi.org/10.3390/POLYM13142363
2. Al-Rumaihi, A., Parthasarathy, P., Fernandez, A., Al-Ansari, T., Mackey, H.R., Rodriguez, R., Mazza, G., McKay, G., 2021. Thermal degradation characteristics and kinetic study of camel manure pyrolysis. J. Environ. Chem. Eng. 9, 106071. https://doi.org/10.1016/J.JECE.2021.106071
3. Alherbawi, M., Parthasarathy, P., Al-Ansari, T., Mackey, H., McKay, G., 2021. Potential of drop-in biofuel production from camel manure by hydrothermal liquefaction and biocrude upgrading: A Qatar case study. Energy 232, 121027. https://doi.org/10.1016/J.ENERGY.2021.121027
4. Bensidhom, G., Arabiourrutia, M., Ben Hassen Trabelsi, A., Cortazar, M., Ceylan, S., Olazar, M., 2021. Fast pyrolysis of date palm biomass using Py-GCMS. J. Energy Inst. 99, 229–239. https://doi.org/10.1016/J.JOEI.2021.09.012
5. Caballero, J.A., Conesa, J.A., Font, R., Marcilla, A., 1997. Pyrolysis kinetics of almond shells and olive stones considering their organic fractions. J. Anal. Appl. Pyrolysis 42,

159–175. https://doi.org/10.1016/S0165-2370(97)00015-6
6. Caro, S., Dahl, O., 2021. Thermochemical valorisation of waste: Pyrolytic conversion of horse manure. Clean. Eng. Technol. 4, 100181. https://doi.org/10.1016/J.CLET.2021.100181
7. Chandrasekaran, M., Bahkali, A.H., 2013. Valorization of date palm (Phoenix dactylifera) fruit processing by-products and wastes using bioprocess technology - Review. Saudi J. Biol. Sci. 20, 105–120.
8. Channiwala, S.A., Parikh, P.P., 2002. A unified correlation for estimating HHV of solid, liquid and gaseous fuels. Fuel 81, 1051–1063.
9. Cheng, S., Shu, J., Xia, H., Wang, S., Zhang, L., Peng, J., Li, C., Jiang, X., Zhang, Q., 2019. Pyrolysis of Crofton weed for the production of aldehyde rich bio-oil and combustible matter rich bio-gas. Appl. Therm. Eng. 148, 1164–1170. https://doi.org/10.1016/j.applthermaleng.2018.12.009
10. Colpani, D., Santos, V.O., Araujo, R.O., Lima, V.M.R., Tenório, J.A.S., Coleti, J., Chaar, J.S., de Souza, L.K.C., 2022. Bioenergy potential analysis of Brazil nut biomass residues through pyrolysis: Gas emission, kinetics, and thermodynamic parameters. Clean. Chem. Eng. 1, 100002. https://doi.org/10.1016/J.CLCE.2022.100002
11. Demirbas, A., 2017. Utilization of date biomass waste and date seed as bio-fuels source. Energy Sources, Part A Recover. Util. Environ. Eff. https://doi.org/10.1080/15567036.2016.1261208
12. Dhyani, V., Bhaskar, T., 2018. Kinetic Analysis of Biomass Pyrolysis, in: Bhaskar, T., Pandey, A., Mohan, S.V., Lee, D.-J., Khanal, S. (Eds.), Waste Biorefinery Potential and Perspectives. Elsevier, Amsterdam, Netherlands, pp. 39–83.
13. Di Blasi, C., 2008. Modeling chemical and physical processes of wood and biomass pyrolysis. Prog. Energy Combust. Sci. 34, 47–90.
14. El may, Y., Jeguirim, M., Dorge, S., Trouvé, G., Said, R., 2012. Study on the thermal behavior of different date palm residues: Characterization and devolatilization kinetics under inert and oxidative atmospheres. Energy 44, 702–709. https://doi.org/10.1016/J.ENERGY.2012.05.022
15. Fadhil, A.B., Alhayali, M.A., Saeed, L.I., 2017. Date (Phoenix dactylifera L.) palm stones as a potential new feedstock for liquid bio-fuels production. Fuel 210, 165–176. https://doi.org/10.1016/J.FUEL.2017.08.059
16. Fadhil, A.B., Kareem, B.A., 2021. Co-pyrolysis of mixed date pits and olive stones: Identification of bio-oil and the production of activated carbon from bio-char. J. Anal. Appl. Pyrolysis 158, 105249. https://doi.org/10.1016/J.JAAP.2021.105249
17. FAO, 2020. Proposal for an international year of date palm [WWW Document]. Food Agric. Organ. URL http://www.fao.org/3/nd415en/nd415en.pdf
18. Fernandez, A., Mazza, G., Rodriguez, R., 2018. Thermal decomposition under oxidative atmosphere of lignocellulosic wastes: Different kinetic methods application. J. Environ. Chem. Eng. 6, 404–415. https://doi.org/10.1016/j.jece.2017.12.013
19. Fernandez, A., Ortiz, L.R., Asensio, D., Rodriguez, R., Mazza, G., 2020. Kinetic analysis and thermodynamics properties of air/steam gasification of agricultural waste. J. Environ. Chem. Eng. 8, 103829. https://doi.org/10.1016/j.jece.2020.103829
20. Fernandez, A., Saffe, A., Pereyra, R., Mazza, G., Rodriguez, R., 2016. Kinetic study of regional agro-industrial wastes pyrolysis using non-isothermal TGA analysis. Appl. Therm. Eng. 106, 1157–1164. https://doi.org/10.1016/j.applthermaleng.2016.06.084

21. Giwa, A.S., Xu, H., Wu, J., Li, Y., Chang, F., Zhang, X., Jin, Z., Huang, B., Wang, K., 2018. Sustainable recycling of residues from the food waste (FW) composting plant via pyrolysis: Thermal characterization and kinetic studies. J. Clean. Prod. 180, 43–49. https://doi.org/10.1016/j.jclepro.2018.01.122
22. Goenka, R., Parthasarathy, P., Gupta, N.K., Biyahut, N.K., Sheeba, K.N., 2015. Kinetic analysis of biomass and comparison of its chemical compositions by thermogravimetry, wet and experimental furnace methods. Waste and Biomass Valorization 6, 989–1002. https://doi.org/10.1007/s12649-015-9402-3
23. Guan, Y., Liu, C., Peng, Q., Zaman, F., Zhang, H., Jin, Z., Wang, A., Wang, W., Huang, Y., 2019. Pyrolysis kinetics behavior of solid leather wastes. Waste Manag. 100, 122–127. https://doi.org/10.1016/j.wasman.2019.09.005
24. Guo, X., Xu, Z., Zheng, X., Jin, X., Cai, J., 2022. Understanding pyrolysis mechanisms of corn and cotton stalks via kinetics and thermodynamics. J. Anal. Appl. Pyrolysis 164, 105521. https://doi.org/10.1016/J.JAAP.2022.105521
25. Gupta, N.K., Prakash, P., Kalaichelvi, P., Sheeba, K.N., 2016. The effect of temperature and hemicellulose-lignin, cellulose-lignin, and cellulose-hemicellulose on char yield from the slow pyrolysis of rice husk. Energy Sources, Part A Recover. Util. Environ. Eff. 38, 1428–1434. https://doi.org/10.1080/15567036.2014.941518
26. Heydari, M., Rahman, M., Gupta, R., 2015. Kinetic study and thermal decomposition behavior of lignite coal. Int. J. Chem. Eng. 2015. https://doi.org/10.1155/2015/481739
27. Hijab, M., Parthasarathy, P., Mackey, H.R., Al-Ansari, T., McKay, G., 2021. Minimizing adsorbent requirements using multi-stage batch adsorption for malachite green removal using microwave date-stone activated carbons. Chem. Eng. Process. - Process Intensif. 167, 108318. https://doi.org/10.1016/J.CEP.2021.108318
28. Islam, M.A., Auta, M., Kabir, G., Hameed, B.H., 2016. A thermogravimetric analysis of the combustion kinetics of karanja (Pongamia pinnata) fruit hulls char. Bioresour. Technol. 200, 335–341. https://doi.org/10.1016/j.biortech.2015.09.057
29. Junhui Zhang, Liu, J., Evrendilek, F., Zhang, X., Buyukada, M., 2019. TG-FTIR and Py-GC/MS analyses of pyrolysis behaviors and products of cattle manure in CO2 and N2 atmospheres: Kinetic, thermodynamic, and machine-learning models. Energy Convers. Manag. 195, 346–359.
30. Kumar, A., Monika, Mishra, R.K., jaglan, S., 2022. Pyrolysis of low-value waste miscanthus grass: Physicochemical characterization, pyrolysis kinetics, and characterization of pyrolytic end products. Process Saf. Environ. Prot. 163, 68–81. https://doi.org/10.1016/J.PSEP.2022.05.022
31. Marion Carrier, Loppinet-Serani, A., Denux, D., Lasnier, J.-M., Ham-Pichavant, F., Cansell, F., Aymonier, C., 2011. Thermogravimetric analysis as a new method to determine the lignocellulosic composition of biomass. Biomass and Bioenergy 35, 298–307.
32. Ming, X., Xu, F., Jiang, Y., Zong, P., Wang, B., Li, J., Qiao, Y., Tian, Y., 2020. Thermal degradation of food waste by TG-FTIR and Py-GC/MS: Pyrolysis behaviors, products, kinetic and thermodynamic analysis. J. Clean. Prod. 244, 118713. https://doi.org/10.1016/J.JCLEPRO.2019.118713
33. Mishra, G., Bhaskar, T., 2014. Non isothermal model free kinetics for pyrolysis of rice straw. Bioresour. Technol. 169, 614–621. https://doi.org/10.1016/J.BIORTECH.2014.07.045

34. Mishra, R.K., Mohanty, K., 2020. Kinetic analysis and pyrolysis behaviour of waste biomass towards its bioenergy potential. Bioresour. Technol. 311, 123480. https://doi.org/10.1016/J.BIORTECH.2020.123480
35. Müsellim, E., Tahir, M.H., Ahmad, M.S., Ceylan, S., 2018. Thermokinetic and TG/DSC-FTIR study of pea waste biomass pyrolysis. Appl. Therm. Eng. 137, 54–61. https://doi.org/10.1016/j.applthermaleng.2018.03.050
36. Otero, M., Lobato, A., Cuetos, M.J., Sánchez, M.E., Gómez, X., 2011. Digestion of cattle manure: Thermogravimetric kinetic analysis for the evaluation of organic matter conversion. Bioresour. Technol. 102, 3404–3410. https://doi.org/10.1016/j.biortech.2010.10.016
37. Özsin, G., Pütün, A.E., 2019. TGA/MS/FT-IR study for kinetic evaluation and evolved gas analysis of a biomass/PVC co-pyrolysis process. Energy Convers. Manag. 182, 143–153. https://doi.org/10.1016/J.ENCONMAN.2018.12.060
38. Parthasarathy, P., Al-Ansari, T., Mackey, H.M., McKay, G., 2021. Effect of heating rate on the pyrolysis of camel manure. Biomass Convers. Biorefinery 2021 1–13. https://doi.org/10.1007/S13399-021-01531-9
39. Parthasarathy, P., Narayanan, K.S., Arockiam, L., 2013. Study on kinetic parameters of different biomass samples using thermo-gravimetric analysis. Biomass and Bioenergy 58, 58–66. https://doi.org/10.1016/j.biombioe.2013.08.004
40. Parthasarathy, P., Narayanan, K.S., Ceylan, S., Pambudi, N.A., 2017. Optimization of parameters for the generation of hydrogen in combined slow pyrolysis and steam gasification of biomass. Energy and Fuels 31, 13692–13704. https://doi.org/10.1021/acs.energyfuels.7b02429
41. Prakash, P., Sheeba, K.N., 2016. Prediction of pyrolysis and gasification characteristics of different biomass from their physico-chemical properties. Energy Sources, Part A Recover. Util. Environ. Eff. 38, 1530–1536. https://doi.org/10.1080/15567036.2014.953713
42. PSA, 2018. Agriculture Statistics, Planning and Statistics Authority (PSA), Qatar. Doha.
43. Ro, K.S., Cantrell, K.B., Hunt, P.G., 2010. High-Temperature Pyrolysis of Blended Animal Manures for Producing Renewable Energy and Value-Added Biochar. Ind. Eng. Chem. Res. 49, 10125–10131. https://doi.org/10.1021/IE101155M
44. Sait, H.H., Hussain, A., Salema, A.A., Ani, F.N., 2012. Pyrolysis and combustion kinetics of date palm biomass using thermogravimetric analysis. Bioresour. Technol. 118, 382–389. https://doi.org/10.1016/J.BIORTECH.2012.04.081
45. Sánchez, M.E., Martínez, O., Gómez, X., Morán, A., 2007. Pyrolysis of mixtures of sewage sludge and manure: A comparison of the results obtained in the laboratory (semi-pilot) and in a pilot plant. Waste Manag. 27, 1328–1334. https://doi.org/10.1016/J.WASMAN.2006.07.015
46. Shim, J.W., Pyo, S., Lam, S.S., Jae, J., Jeon, B.H., Khan, M.A., Lin, K.Y.A., Kim, Y.M., Jung, S.C., Park, Y.K., 2022. Catalytic pyrolysis of chicken manure over various catalysts. Fuel 322, 124241. https://doi.org/10.1016/J.FUEL.2022.124241
47. Singh, D.K., Tirkey, J. V., 2021. Modeling and multi-objective optimization of variable air gasification performance parameters using Syzygium cumini biomass by integrating ASPEN Plus with Response surface methodology (RSM). Int. J. Hydrogen Energy 46, 18816–18831. https://doi.org/10.1016/J.IJHYDENE.2021.03.054
48. Wang, Y., Yuan, T., Zhang, Z., Lei, Z., Shimizu, K., 2020. Improved lignocellulose

degradation prior to semi-dry anaerobic digestion of dairy manure via potassium permanganate treatment. Bioresour. Technol. Reports 11, 100462. https://doi.org/10.1016/J.BITEB.2020.100462

49. Wzorek, M., Junga, R., Yilmaz, E., Niemiec, P., 2021. Combustion behavior and mechanical properties of pellets derived from blends of animal manure and lignocellulosic biomass. J. Environ. Manage. 290, 112487. https://doi.org/10.1016/J.JENVMAN.2021.112487
50. Xu, Y., Qi, F., Bai, T., Yan, Y., Wu, C., An, Z., Luo, S., Huang, Z., Xie, P., 2019. A further inquiry into co-pyrolysis of straws with manures for heavy metal immobilization in manure-derived biochars. J. Hazard. Mater. 380, 120870. https://doi.org/10.1016/J.JHAZMAT.2019.120870
51. Yuan, X., He, T., Cao, H., Yuan, Q., 2017. Cattle manure pyrolysis process: Kinetic and thermodynamic analysis with isoconversional methods. Renew. Energy 107, 489–496. https://doi.org/10.1016/j.renene.2017.02.026
52. Zhu, Y., Merbold, L., Leitner, S., Pelster, D.E., Okoma, S.A., Ngetich, F., Onyango, A.A., Pellikka, P., Butterbach-Bahl, K., 2020. The effects of climate on decomposition of cattle, sheep and goat manure in Kenyan tropical pastures. Plant Soil 451, 325–343.